



**CHALMERS**  
UNIVERSITY OF TECHNOLOGY

## **Characterization from Diesel and Renewable Fuel Engine Exhaust: Particulate Size/Mass Distributions and Optical Properties**

Downloaded from: <https://research.chalmers.se>, 2026-04-05 05:17 UTC

Citation for the original published paper (version of record):

Sharma, N., Mitra, K., Pezer, J. et al (2023). Characterization from Diesel and Renewable Fuel Engine Exhaust: Particulate Size/Mass Distributions and Optical Properties. *Aerosol Science and Engineering*, 7: 182-191.  
<http://dx.doi.org/10.1007/s41810-023-00172-x>

N.B. When citing this work, cite the original published paper.



# Characterization from Diesel and Renewable Fuel Engine Exhaust: Particulate Size/Mass Distributions and Optical Properties

Nikhil Sharma<sup>1</sup> · Kalyan Mitra<sup>2</sup> · Jelena Pezer<sup>2</sup> · Ravikant Pathak<sup>2</sup> · Jonas Sjöblom<sup>3</sup>

Received: 31 August 2022 / Revised: 25 November 2022 / Accepted: 2 January 2023  
© The Author(s) 2023

## Abstract

Combustion of fossil fuel produces emissions and is one of the major environmental problems leading to climate change. Diesel engines are highly efficient but produce particulate emissions. These particulate emissions are considered dangerous to human health because inhaling particulates may cause respiratory and heart disease. Substituting fossil diesel fuel with renewable diesel fuel and using diesel particulate filters is one possibility to meet stringent legislative requirements. With this motivation, the present experimental investigation aimed to evaluate the particle size distribution (PSD), optical properties of particulate matter (PM) emitted, and the outcome of using an after-treatment system comprising of a diesel particle filter (DPF). This investigation aimed to make a comparative analysis of particulate emission upstream and downstream of the DPF with and without ultraviolet (UV) light (405 nm and 781 nm wavelength) turned on/off. Experiments were performed at (a) engine idle with a torque of 6 Nm at 750 rpm, IMEP of 1.35 bar and power of 0.5 kW, (b) engine at part load with a torque of 32 Nm at 1200 rpm, IMEP of 8.5 bar and power of 4.5 kW. Diesel engine was operated on two fuels (a) Diesel and (b) EHR7. Results showed that as and when UV light was turned on, a distinct nucleation mode that dominated the number concentration for both test fuels were observed. Downstream of the filter had relatively higher AAE values which show the contribution to climate change. Present experimental research is important for renewable fuel industries, industrial innovation's future, and the exhaust gas after-treatment system (EATS) community. The results contribute to knowledge for occupational exposure, human health, and the environment.

**Keywords** Particle aging · Oxygenated fuel · Particle number size distribution · UV Light · DPF

## Abbreviations

AAE Ångström absorption exponent  
BC Black carbon  
BrC Brown carbon  
BSFC Brake-specific fuel consumption  
CAD Crank angle degree  
CN Cetane number

CO Carbon monoxide  
CO<sub>2</sub> Carbon dioxide  
CRDI Common rail direct injection  
DOC Diesel oxidation catalyst  
Dp Particle size  
DPF Diesel particle filter  
EATS Exhaust gas after-treatment system  
EC Elemental carbon  
EGR Exhaust gas recirculation  
EHR7 37% 2-Ethylhexanol + 56% HVO + 7% RME by volume  
Go:PAM Gothenburg Potential Aerosol Mass chamber  
HC Hydrocarbon  
IMEP Indicated mean effective pressure  
kW Kilowatt  
LHV Lower heating value  
MSS Micro soot sensor  
NOx Nitrogen oxides  
O<sub>3</sub> Ozone  
PAH Polycyclic aromatic hydrocarbon

✉ Ravikant Pathak  
ravikant@chem.gu.se

✉ Jonas Sjöblom  
jonas.sjoblom@chalmers.se

<sup>1</sup> Department of Mechanical Engineering, Malaviya National Institute of Technology Jaipur, Jaipur, Rajasthan 302017, India

<sup>2</sup> Division of Combustion and Propulsion Systems, Department of Mechanics and Maritime Sciences, Chalmers University of Technology, Gothenburg, Sweden

<sup>3</sup> Department of Chemistry and Molecular Science, Gothenburg University, Gothenburg, Sweden

PASS-3	Photoacoustic soot spectrometer
PM	Particulate matter
PN	Particle number
PSD	Particle size distribution
rpm	Revolutions per minute
SMPS	Scanning mobility particle sizer
SOA	Secondary organic aerosol
UFP	Ultrafine particles
UV	Ultraviolet

## 1 Introduction

The worldwide demand for transport energy is large and is growing every year despite of development in electric vehicles (Liu et al. 2022; Lebrouhi et al. 2021; Chia et al. 2022). Diesel engines offer numerous advantages over other power plants and are prevalent in the industrial, agricultural, heavy-duty transport sectors and commercial establishments (Sharma et al. 2022; Reddy et al. 2018; Hoang 2021). These advantages include higher power output, higher thermal efficiency, higher torque, better durability, and superior brake-specific fuel consumption (BSFC). But diesel engine exhaust is known to promote air pollution, climate change/global warming, cardiovascular disease, and lung cancer (Somasundaram et al. 2020; Franklin et al. 2015; Riddle et al. 2007; Bikis and Pandey 2022). Use of renewable fuel coupled with diesel particulate filter (DPF) technology can suppress these issues (Gren et al. 2021). Fuel prices are high and scientists are exploring cost-effective renewable fuel to meet emission legislation and reduce dependence upon foreign crude oil and ensure the security of the supply (Jaber et al. 2004; Wu et al. 2012).

Significant effort has been made to regulate the emissions from the transportation sector. Amongst the various PM characteristics, PM mass, number, and size are vital parameters for research. Particles have a high retention time in the atmosphere causing high risk to the human respiratory system (Wang et al. 2021). PM physical, and PM chemical properties affect soot. These properties are important for DPF investigations. PM can be classified based on its size, as a combination of individual particles as coarse, fine and ultrafine particles. Ultrafine particles (UFPs; diameter less than 100 nm) can increase the risk of asthma attacks, heart disease and lung cancer (Sharma and Agarwal 2017). Smaller size particles are of concern as these are large in number but have insignificant mass. Due to higher number concentration and comparatively large surface area (for same mass), they may affect the human respiratory system. Soot can be classified as black carbon (BC) or brown carbon (BrC), and they have a different amount of contributions to climate change (Wu et al. 2016). In recent years, BrC has attracted interest among researchers as a possible cause of

climate change (Wu et al. 2016; Yan et al. 2018; Pani et al. 2021; Zhu et al. 2021). Renewable fuels are known to have low aromatic content in them compared to conventional fuel such as diesel. This property of renewable fuel potentially reduce the formation of SOA (Gentner et al. 2017). In the fast few decades, consumption of renewable fuel has increased but knowledge about the impact of SOA formation is limited (Gentner et al. 2017). Hence, evaluating climate-relevant optical properties of the particulate matter (PM) upstream and downstream of the DPF is essential (Preuß et al. 2018). BC or soot is one of the critical combustion-generated particles. It originates primarily from diesel/gasoline that absorbs light over the entire visible spectrum (Hansen et al. 1984). BC is generated by the incomplete combustion of fuels and is used as a tracer for combustion. Liu et al. (2018a) characterized the chemical composition of particulate matter from heavy-duty trucks and construction equipment fueled with conventional diesel fuel. Authors reported that the highest quantity of PM<sub>2.5</sub> was contributed by carbonaceous matter. Emissions from the diesel engine are mainly composed of carbon di-oxide (CO<sub>2</sub>), carbon monoxide (CO), nitrogen oxides (NO<sub>x</sub>), gaseous hydrocarbons (HC), and of particulate matter (Maricq 2007). Corbin et al. (2018) investigated the optical properties of particulate emission from marine engines operating on heavy fuel oil and distillate fuels. In this, the authors focused on “brown carbon” light absorption characteristics of soot. DOCs can oxidize more than 70% of the CO and HCs from diesel engines and therefore is positioned upstream of DPF (Wei et al. 2015; Caliskan and Mori 2017). Carbon monoxide (CO) is a toxic, odorless, and colorless air pollutant which is a poisonous atmospheric pollutant affecting human beings, plants, animals and environment (Dey and Dhal 2019). Yadav et al. (2021) performed an experimental investigation to estimate the sources and health risks of PM<sub>2.5</sub> PAHs and the carbonaceous species environment of Delhi. Authors reported carcinogenic PAHs put up-41.4% to the aerosol PAHs load in the Delhi atmosphere. Caliskan and Mori (2017) reported that oxidation of soot occurs at higher temperature and changes soot morphologies. Glassman (Smith 1981) reported that soot oxidation happens when the temperature is greater than 1300 K. Soot mostly comprises elemental carbon (EC) arranged in graphitic-like material (Kittelson 1998). Chen et al. (2019) have investigated the characteristics of PM and correlated the emitted smoke opacity and soot emissions from a turbo-charged and intercooled diesel engine fueled with methanol/diesel dual fuel. They reported an increase in the level of soot and PM with an increase in methanol fraction at high air intake temperature and, high engine loads. However, a decrease in soot and PM level was reported at high engine load with lesser air intake temperature. In another study, Liu et al. (2014) experimentally investigated the influence of methanol fraction and injection timing on the emissions

characteristics of a six-cylinder heavy-duty diesel engine. Authors reported that with an increase in methanol fraction the trade-off relation between  $\text{NO}_x$  and soot emissions can be optimized in the engine.

Many studies have been conducted on the PSD, and most of these are based on upstream of DPF. There exists a research gap for investigating PSD downstream of the filter in the presence of UV light with respect to ultrafine particles. This experimental investigation aims to compare PSD from diesel and renewable fuel sampled at medium load and engine idle conditions downstream of the DPF. These measurements were done upstream and downstream of the DPF. Experiments were performed at (a) engine idle with a torque of 6 Nm at 750 rpm, IMEP of 1.35 bar and power of 0.5 kW, (b) engine at part load with a torque of 32 Nm at 1200 rpm, IMEP of 8.5 bar, and power of 4.5 Kw. Diesel engine was operated on two fuels (a) Diesel (b) Renewable (EHR7).

## 2 Experimental Setup and Methodology

### 2.1 Experimental Setup

An experimental investigation was performed on a single-cylinder (Ricardo hydra) common rail direct injection (CRDI) engine coupled with a Denso injector. This Ricardo hydra engine was fitted with a Volvo NED4 cylinder head. Figure 1 shows the engine schematic, and Table 1 shows the engine specifications. The Denso injector was capable of producing four injections per cycle. A pressure transducer

**Table 1** Test engine specifications

Engine type	Ricardo Hydra
Engine head	Volvo NED4
Displaced volume, $\text{dm}^3$	0.49
Bore, mm	82
Stroke, mm	93
Compression ratio	15.8: 1
Fuel injection system	Common rail direct injection

(AVL GUI2S-10) was used to measure in-cylinder pressure signals. The experimental setup also includes a pressure signal/piezo charge amplifier (Kistler 5011) was also part of the experimental setup. A combustion analyzer (AVL IndiCom) detected the pressure signal with a resolution of 0.2 CAD. The amount of fuel injected in each cycle was measured by a fuel metering unit (AVL 730). EGR percentage was calculated using the proportion of the carbon dioxide emission in the exhaust.

### 2.2 Particulate Measurement

Gothenburg Potential Aerosol Mass chamber (Go:PAM) was coupled with engine exhaust as the photo-oxidation reaction zone (Tsiligiannis et al. 2019). OH radicals were formed using Go:PAM by photolyzing  $\text{O}_3$ . This was done in the presence of water vapor. In addition to this, total flows

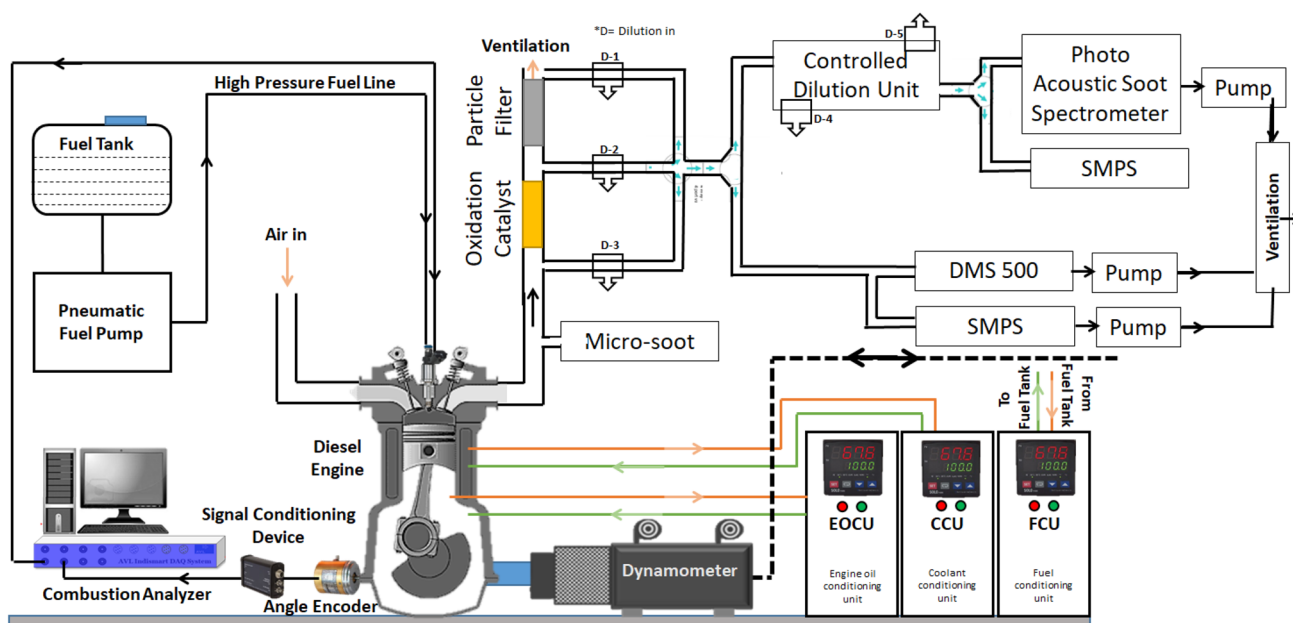


**Fig. 1** Schematic of the experimental setup

through the apparatus were measured and SOA was formed in a laminar flow. A SMPS (CPC 3775; EC3080 TSI Inc. Shoreview, MN, USA) was part of the experimental setup used to quantify the PN concentration and volume concentration of SOA inside the sample outflow line. The absorption and scattering properties of SOA were characterized using 3-wavelength photoacoustic soot spectrometer (PASS-3). Details about both instruments can be referred at Bäckström et al. (2017). AVL Micro Soot Sensor (MSS plus) was part of the experimental setup and used to measure the mass of particulate per cubic meter in the exhaust pipe.

*EATS*: Exhaust gas after-treatment system consists of an oxidation catalyst followed by a DPF. A temperature of 250 °C was maintained in the exhaust gas after-treatment system. A differential pressure sensor was placed across the particulate filter to measure the real-time pressure drop during PSD measurement.

### 2.3 Test Fuels

Diesel and EHR7 were used as test fuel for this experimental investigation. The selection of the blended fuel was considered to mimic the properties of diesel with respect to cetane number (CN). Detailed properties and composition are listed in Table 2.

### 2.4 Experimental Procedure

While collecting the exhaust samples, it was ensured that soot was a representative sample and the engine had achieved a steady-state condition. Engine was operated at 6.5 Nm@750 rpm and 32 Nm load@1200 rpm with an ERG percentage of  $19 \pm 0.3\%$ . Denso injector was used with two pre-injections followed by one main and one post-injection in one engine operating cycle. A constant fuel injection pressure of  $817.6 \pm 0.6$  bar was maintained throughout the experiment. The lower heating value (LHV) of oxygenated fuel was compensated by

**Table 2** Test fuel composition and properties

Property	Unit	Diesel	EHR7
2-Ethylhexanol content	vol%	–	37
Diesel content	vol%	100	–
HVO content	vol%	–	56
RME content	vol%	–	7
Oxygen content	m%	0	5.4
H/C ratio	[–]	1.833	2.137
O/C ratio	[–]	–	0.043
Lower heating value	MJ/kg	42.9	41.12
Density	kg/m <sup>3</sup>	830	806.4
CN	[–]	52	51.3

keeping the injection duration slightly longer and a fixed injection start. Water was used as a coolant in the engine, and the temperature of coolant  $T_{in}$  (into the engine) was maintained at 73 °C, and  $T_{out}$  was maintained (out of the engine) was 79 °C.

Table 3 shows the experimental matrix and run order for particulate measurement.

Table 3 shows the experimental matrix in detail. Experiments were performed at (a) engine idle with torque of 6 Nm at 750 rpm, IMEP of 1.35 bar and power of 0.5 Kw, (b) engine at part load with torque of 32 Nm at 1200 rpm, IMEP of 8.5 bar and power of 4.5 kW.

## 3 Results and Discussion

Results will be discussed in terms of particle number size distribution, particle mass size distribution, total particle number and mass emission, engine soot emissions and Ångström absorption exponent (AAE).

**Table 3** Experimental Matrix

S. no.	Fuel	Load	Position	UV Light	Run order
1	Diesel	Part load	Upstream	Off	5
2	Diesel	Part load	Upstream	On	6
3	Diesel	Part load	Down-stream	Off	7
4	Diesel	Part load	Down-stream	On	8
5	Diesel	Engine Idle	Upstream	Off	1
6	Diesel	Engine Idle	Upstream	On	2
7	Diesel	Engine Idle	Down-stream	Off	3
8	Diesel	Engine Idle	Down-stream	On	4
9	Renewable fuel	Part load	Upstream	Off	13
10	Renewable fuel	Part load	Upstream	On	14
11	Renewable fuel	Part load	Down-stream	Off	15
12	Renewable fuel	Part load	Down-stream	On	16
13	Renewable fuel	Engine Idle	Upstream	Off	9
14	Renewable fuel	Engine Idle	Upstream	On	10
15	Renewable fuel	Engine Idle	Down-stream	Off	11
16	Renewable fuel	Engine Idle	Down-stream	On	12

### 3.1 Particle Number Size Distribution

Figure 2 shows PN emissions at the engine’s part load condition, upstream and downstream of the filter with UV light on and off. Figure 2a and b shows, comparison among diesel and renewable fuel. Figure 2c and d shows, comparison among the upstream and downstream of filter. Nucleation mode particles (< 20 nm) dominated the number concentration. Soot mode particles (~ 100 nm) dominated the total emitted mass. In Fig. 2, nucleation mode particle contributed to the number emission but their contribution to mass emission was less (refer Fig. 5). As and when UV light was turned on, a distinct nucleation mode that dominated the number concentration for both the test fuels were observed. When UV light was turned off, nucleation mode particles decreased significantly. This large increase in nucleation mode particle was observed at both upstream and downstream of the filter when UV light was turned on. Downstream of the filter PN emission is being barely distinguishable above the background concentrations. But this is not true when UV light is turned on downstream of the filter. Downstream of the filter, the nucleation mode of a particle is relatively less compared to upstream of the filter when UV light is on. Downstream of the filter, when UV light is turned off, PN emission was found to be negligible. Upstream of the filter, when UV light was turned off, as expected, PN emission was found to be slightly higher. These trends were consistent for both the test fuels. However, oxygenated fuel

showed PN emission marginally lower when UV light was turned on. With oxygenated fuel, peak of particulate size-number distribution marginally shifted towards smaller particle sizes ( $D_p$  less than 100 nm). The difference in PN emission with UV light on for upstream and downstream of the filter decreased as the particle size decreases.

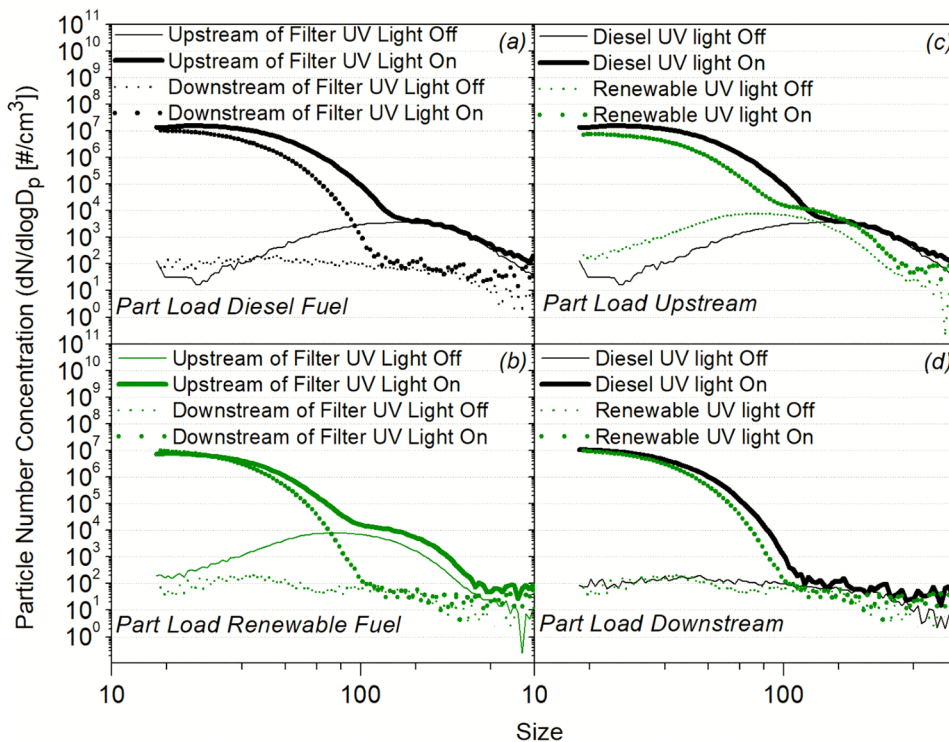
Figure 3 shows PN emissions at engine idle condition upstream and downstream of the filter with UV light on and off. PSD data downstream of the filter, with UV light on was not recorded. The trends in the results are similar to those reported in Fig. 2. However, PN emissions of engine idle are one order magnitude smaller compared to engine part load condition.

Figure 4 shows the total particle number emissions for part load and engine idle conditions.

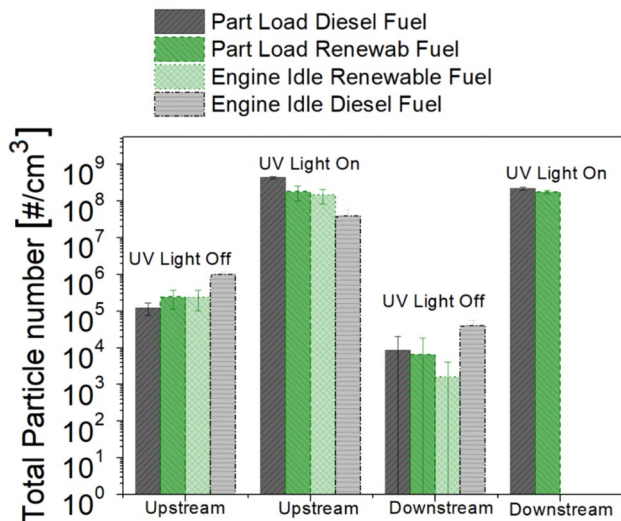
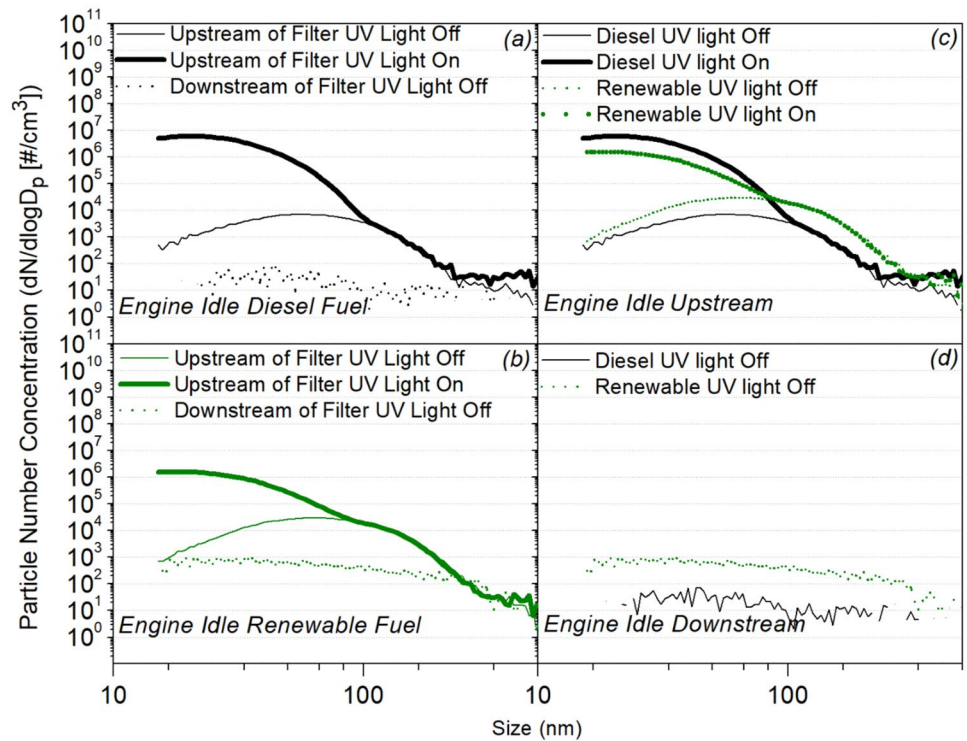
Total particle number emission upstream of the filter was relatively higher compared to downstream of the filter for corresponding light on/off condition. When UV light was turned on, total particle emission was relatively higher. In general, total particle emission for renewable fuel was slightly lower.

Figure 5 shows particle mass size distribution at engine part load condition. As and when UV light was turned on, a relatively higher particle mass emission was observed. As and when UV light was turned off particle mass emission was found to be decreased significantly. The higher particle mass was observed at upstream and downstream of the filter when UV light is turned on. Downstream of the

**Fig. 2** Particle number size distribution vs particle diameter (nm) at engine’s part load



**Fig. 3** Particle number size distribution vs particle diameter (nm) at engine idle



**Fig. 4** Total particle number emission

filter, particle mass emission was relatively less compared to upstream of the filter, when UV light was turned on. Downstream of the filter, when UV light was turned off, particle mass emission was negligible. These trends were consistent for both the test fuels. However, oxygenated fuel showed particle mass emission marginally lower when UV light is turned on. With oxygenated fuel, peak of particulate size-number distribution shifted towards smaller particle sizes ( $D_p \sim 100$  nm). The difference in PN emission with UV light

on for upstream of the filter decreased as the particle size decreased. It should be noted that mass emission for larger size particle, when UV light turned on was relatively higher downstream of the filter.

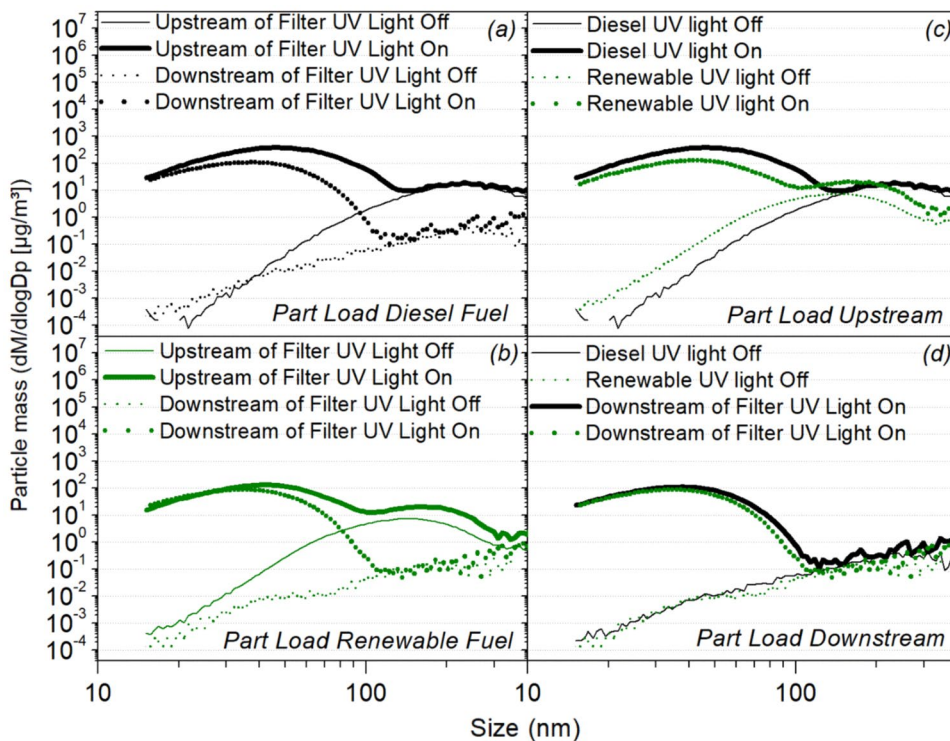
Figure 6 shows particle mass emissions at engine idle condition upstream and downstream of the filter with UV light on and off. Data downstream of the filter after with UV light on was not recorded. The trends in the results are similar to those reported in Fig. 3. However, particle mass emissions of engine idle are one order smaller compared to engine part load condition.

Figure 7 shows total particle mass emissions for part load and engine idle conditions. Total particle mass emission upstream of the filter was relatively higher compared to downstream of the filter. In addition it, “UV light on” had comparatively higher particle mass emission.

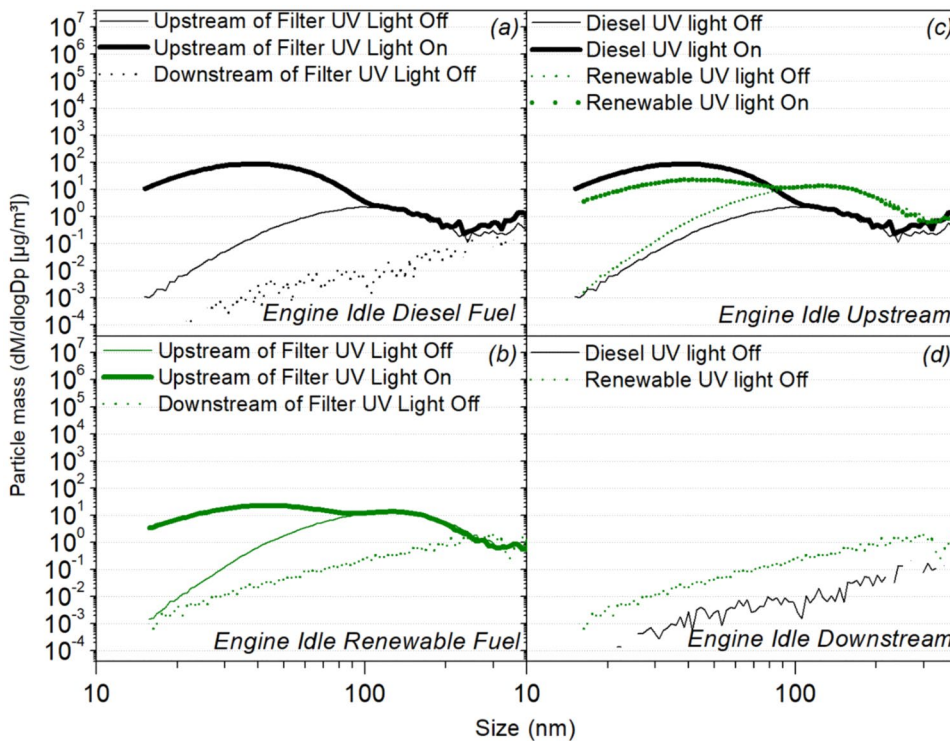
Figure 8 shows soot mass emissions from the engine idle and engine part load operating condition. Microsoot was used to capture soot in g/kW-h. It was found that soot from diesel fuel was relatively higher for part load compared to soot from renewable fuel.

The AAE describes the spectral dependence of light absorption by BC and BrC aerosols. This in-turn governs their influence on climate change, and AAE attribution method is utilized to differentiate the contributions made from two species of light absorption. Obtaining accurate value of AAE has been proven by scientists to be challenging in literature (Wang et al. 2020). Figure 9 shows AAE for part load and engine idle conditions at the upstream

**Fig. 5** Particle mass distribution vs size at engine part load



**Fig. 6** Particle mass distribution vs particle mobility diameter (nm) at engine idle



and downstream of the filter. The AAE of black carbon (BC) particles between 405 and 781 nm is widely accepted to be 1.0, although observational estimates give quite a wide range of 0.6–1.3 (Liu et al. 2018b). In a first comparison among different engine loads, part load engine

operation resulted in significantly higher AAE values relative to engine idle operation at both upstream and downstream of the DPF. In another comparison at the same engine load but different test fuels, renewable

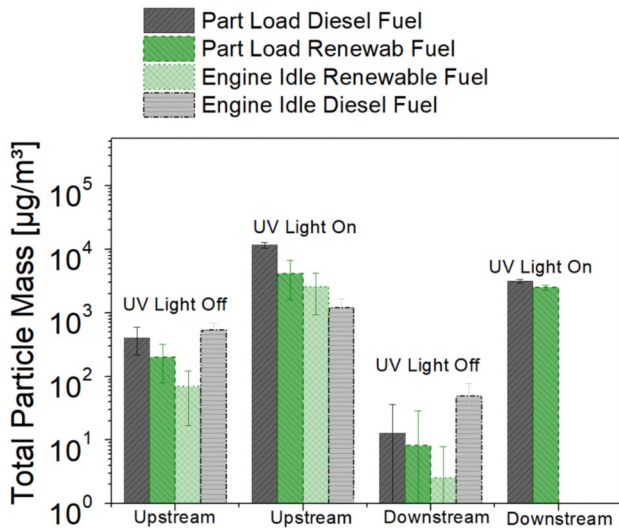


Fig. 7 Total particle number emission

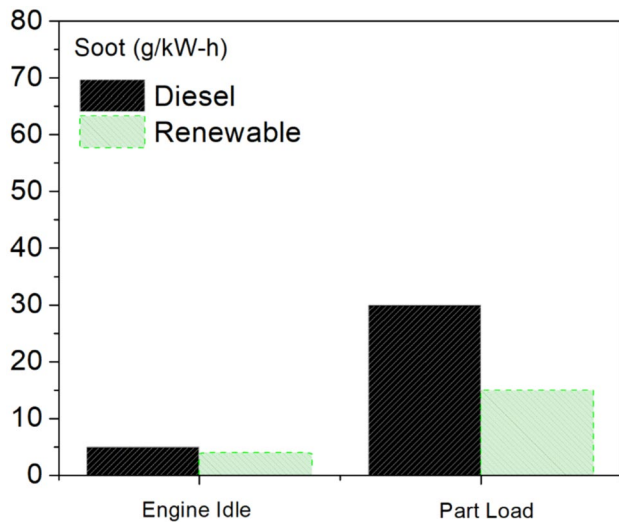


Fig. 8 Soot mass emitted (g/kWh) at part load and engine idle for diesel and renewable fuel

fuel consistently resulted in slightly higher AAE values throughout the test matrix although not statistically significant.

Sources of diesel emissions are ships, trains, and trucks that operate in and around ports. The experimental results give an indication that exposure to diesel exhaust downstream of the filter has important public health implications. A large number of people are exposed to higher diesel exhaust concentrations. Emissions downstream of the filter had relatively higher AAE values which show the contribution to climate change. Implication of this study suggests policy maker to further control the measurement of diesel

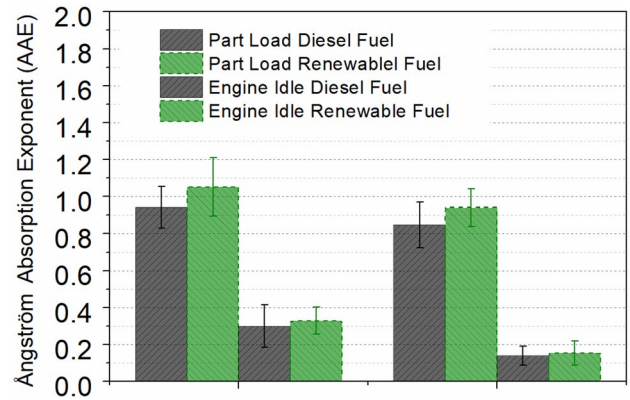


Fig. 9 Ångström absorption exponent (AAE) Upstream the filter (left side) and downstream the filter (right side)

exhaust as particulate emission downstream of the filter may affect individual health if inhaled.

## 4 Conclusions

Diesel engine was operated on two fuels (a) and (b) EHR7. PSD was measured upstream and downstream of the filter with UV light on/off. This experimental investigation emphasis on the contribution of particle emission downstream of the filter to climate changes. Some of the important conclusions are as follows:

- As and when UV light was turned on, a distinct nucleation mode that dominated the number concentration for both fuels were observed.
- With oxygenated fuel, peak of particulate size-number distribution shifted towards smaller particle sizes ( $D_p$  less than 100 nm).
- PN emissions of engine idle are one order smaller compared to engine part load condition.
- Downstream of the filter had relatively higher AAE values which show the contribution to climate change.
- Replacing Diesel with EHR7 decreased the primary particle mass emissions. HVO fuel is sustainable from a climate viewpoint; present experimental investigation shows that from a health perception, particle emission downstream of the filter may contribute to climate change to some extent.

Although the PSD and light-absorbing properties are sensitive to engine operating conditions, fuel type, etc., this manuscript provides a significant improvement over previously available data. The results contribute to knowledge of occupational exposure, human health, and the environment.

**Supplementary Information** The online version contains supplementary material available at <https://doi.org/10.1007/s41810-023-00172-x>.

**Acknowledgements** Efforts made by Dr. Alf-Hugo Magnusson, Dr. Timothy Benham, Robert Buadu and Kristoffer Clasat during the experiments at division of combustion and propulsion systems, department of mechanics and maritime sciences at Chalmers University of Technology, Sweden are acknowledged.

**Author contributions** Conceptualization: JS, RP. Conduct of experiments: JS, NS. Design of experiments: JS. Design of dilution systems: JS, NS. Recording/collection/handling of data: JP, KM, NS, JS. Result analysis and result presentation: NS, JS, RP. NS and JS wrote the first original draft, with contributions from RP. All the authors contributed to proofreading the manuscript.

**Funding** Open access funding provided by Chalmers University of Technology.

**Data availability** The data that support the findings of this study are available from the corresponding author upon reasonable request.

## Declarations

**Conflict of interest** On behalf of all authors, the corresponding authors state that there is no conflict of interest.

**Open Access** This article is licensed under a Creative Commons Attribution 4.0 International License, which permits use, sharing, adaptation, distribution and reproduction in any medium or format, as long as you give appropriate credit to the original author(s) and the source, provide a link to the Creative Commons licence, and indicate if changes were made. The images or other third party material in this article are included in the article's Creative Commons licence, unless indicated otherwise in a credit line to the material. If material is not included in the article's Creative Commons licence and your intended use is not permitted by statutory regulation or exceeds the permitted use, you will need to obtain permission directly from the copyright holder. To view a copy of this licence, visit <http://creativecommons.org/licenses/by/4.0/>.

## References

- Bäckström D, Gunnarsson A, Gall D, Pei X, Johansson R, Andersson K, Pathak RK, Pettersson JB (2017) Measurement of the size distribution, volume fraction and optical properties of soot in an 80 kW propane flame. *Combust Flame* 186:325–334
- Bikis A, Pandey D (2022) Air quality at public transportation stations/stops: contribution of light rail transit to reduce air pollution. *Aerosol Sci Eng* 6:1–16
- Caliskan H, Mori K (2017) Environmental, enviroeconomic and enhanced thermodynamic analyses of a diesel engine with diesel oxidation catalyst (DOC) and diesel particulate filter (DPF) after treatment systems. *Energy* 128:128–144
- Chen C, Yao A, Yao C, Wang B, Lu H, Feng J, Feng L (2019) Study of the characteristics of PM and the correlation of soot and smoke opacity on the diesel methanol dual fuel engine. *Appl Therm Eng* 148:391–403
- Chia SR, Nomanbhay S, Ong MY, Chew KW, Show PL (2022) Renewable diesel as fossil fuel substitution in Malaysia: a review. *Fuel* 314:123137
- Corbin JC, Pieber SM, Czech H, Zanatta M, Jakobi G, Massabò D, Orasche J, El Haddad I, Mensah AA, Stengel B (2018) Brown and black carbon emitted by a marine engine operated on heavy fuel oil and distillate fuels: optical properties, size distributions, and emission factors. *J Geophys Res: Atmos* 123:6175–6195
- Dey S, Dhal GC (2019) A review of synthesis, structure and applications in hopcalite catalysts for carbon monoxide oxidation. *Aerosol Sci Eng* 3:97–131
- Franklin BA, Brook R, Pope CA III (2015) Air pollution and cardiovascular disease. *Curr Probl Cardiol* 40:207–238
- Gentner DR, Jathar SH, Gordon TD, Bahreini R, Day DA, El Haddad I, Hayes PL, Pieber SM, Platt SM, de Gouw J (2017) Review of urban secondary organic aerosol formation from gasoline and diesel motor vehicle emissions. *Environ Sci Technol* 51:1074–1093
- Gren L, Malmberg VB, Falk J, Markula L, Novakovic M, Shamun S, Eriksson AC, Kristensen TB, Svenningsson B, Tunér M (2021) Effects of renewable fuel and exhaust after treatment on primary and secondary emissions from a modern heavy-duty diesel engine. *J Aerosol Sci* 156:105781
- Hansen A, Rosen H, Novakov T (1984) The aethalometer—an instrument for the real-time measurement of optical absorption by aerosol particles. *Sci Total Environ* 36:191–196
- Hoang AT (2021) Combustion behavior, performance and emission characteristics of diesel engine fuelled with biodiesel containing cerium oxide nanoparticles: a review. *Fuel Process Technol* 218:106840
- Jaber JO, Badran O, Abu-Shikhah N (2004) Sustainable energy and environmental impact: role of renewables as clean and secure source of energy for the 21st century in Jordan. *Clean Technol Environ Policy* 6:174–186
- Kittelson DB (1998) Engines and nanoparticles: a review. *J Aerosol Sci* 29:575–588
- Lebrouhi B, Khattari Y, Lamrani B, Maaroufi M, Zeraouli Y, Kouskou T (2021) Key challenges for a large-scale development of battery electric vehicles: a comprehensive review. *J Energy Storage* 44:103273
- Liu J, Yao A, Yao C (2014) Effects of injection timing on performance and emissions of a HD diesel engine with DMCC. *Fuel* 134:107–113
- Liu Y, Zhang W, Yang W, Bai Z, Zhao X (2018a) Chemical compositions of PM<sub>2.5</sub> emitted from diesel trucks and construction equipment. *Aerosol Sci Eng* 2:51–60
- Liu C, Chung CE, Yin Y, Schnaiter M (2018b) The absorption Ångström exponent of black carbon: from numerical aspects. *Atmos Chem Phys* 18:6259–6273
- Liu J, Li M, Zeng Y, Yin M, Zhang X (2022) An improved methodology for evaluating energy service demand for China's passenger transport sector. *Adv Clim Chang Res* 13:290–300
- Maricq MM (2007) Chemical characterization of particulate emissions from diesel engines: a review. *J Aerosol Sci* 38:1079–1118
- Pani SK, Lin N-H, Griffith SM, Chantara S, Lee C-T, Thepnuan D, Tsai YI (2021) Brown carbon light absorption over an urban environment in northern peninsular Southeast Asia. *Environ Pollut* 276:116735
- Preuß J, Munch K, Denbratt I (2018) Performance and emissions of long-chain alcohols as drop-in fuels for heavy duty compression ignition engines. *Fuel* 216:890–897
- Reddy SM, Sharma N, Gupta N, Agarwal AK (2018) Effect of non-edible oil and its biodiesel on wear of fuel injection equipment components of a genset engine. *Fuel* 222:841–851
- Riddle SG, Robert MA, Jakober CA, Hannigan MP, Kleeman MJ (2007) Size distribution of trace organic species emitted from heavy-duty diesel vehicles. *Environ Sci Technol* 41:1962–1969
- Sharma N, Agarwal AK (2017) Effect of the fuel injection pressure on particulate emissions from a gasohol (E15 and M15)-fuelled gasoline direct injection engine. *Energy Fuels* 31:4155–4164
- Sharma N, Preuss J, Sjöblom J (2022) Morphological characterization of soot from a compression ignition engine fueled with

- diesel and an oxygenated fuel. *Int J Engine Res.* <https://doi.org/10.1177/14680874211073938>
- Smith OI (1981) Fundamentals of soot formation in flames with application to diesel engine particulate emissions. *Prog Energy Combust Sci* 7:275
- Somasundaram D, Elango A, Karthikeyan S (2020) Estimation of carbon credits of fishing boat diesel engine running on diesel-ethanol-bio-diesel blends with nano alumina doped ceria-zirconia. *Mater Today: Proc* 33:2923–2928
- Tsiligiannis E, Hammes J, Salvador CM, Mentel TF, Hallquist M (2019) Effect of NO<sub>x</sub> on 1, 3, 5-trimethylbenzene (TMB) oxidation product distribution and particle formation. *Atmos Chem Phys* 19:15073–15086
- Wang Q, Liu H, Ye J, Tian J, Zhang T, Zhang Y, Liu S, Cao J (2020) Estimating absorption Ångström exponent of black carbon aerosol by coupling multiwavelength absorption with chemical composition. *Environ Sci Technol Lett* 8:121–127
- Wang M, Hu T, Wu F, Duan J, Song Y, Zhu Y, Xue C, Zhang N, Zhang D (2021) Characterization of PM<sub>2.5</sub> carbonaceous particles with a high-efficiency SEM: a case study at a suburban area of Xi'an. *Aerosol Sci Eng* 5:70–80
- Wei L, Yao C, Wang Q, Pan W, Han G (2015) Combustion and emission characteristics of a turbocharged diesel engine using high premixed ratio of methanol and diesel fuel. *Fuel* 140:156–163
- Wu G, Liu L-C, Han Z-Y, Wei Y-M (2012) Climate protection and China's energy security: win-win or tradeoff. *Appl Energy* 97:157–163
- Wu G-M, Cong Z-Y, Kang S-C, Kawamura K, Fu P-Q, Zhang Y-L, Wan X, Gao S-P, Liu B (2016) Brown carbon in the cryosphere: current knowledge and perspective. *Adv Clim Chang Res* 7:82–89
- Yadav AK, Sarkar S, Jyethi DS, Rawat P, Aithani D, Siddiqui Z, Khillare P (2021) Fine particulate matter bound polycyclic aromatic hydrocarbons and carbonaceous species in Delhi's atmosphere: seasonal variation, sources, and health risk assessment. *Aerosol Sci Eng* 5:193–213
- Yan J, Wang X, Gong P, Wang C, Cong Z (2018) Review of brown carbon aerosols: Recent progress and perspectives. *Sci Total Environ* 634:1475–1485
- Zhu C-S, Qu Y, Zhou Y, Huang H, Liu H-K, Yang L, Wang Q-Y, Hansen AD, Cao J-J (2021) High light absorption and radiative forcing contributions of primary brown carbon and black carbon to urban aerosol. *Gondwana Res* 90:159–164